

DOI: 10.1002/cmdc.200500035

A Series of Unconjugated Ferrocenyl Phenols: Prospects as Anticancer Agents

Elizabeth Hillard,^[a] Anne Vessières,^[a] Franck Le Bideau,^[a] Damian Plazuk,^[a, b] Daniela Spera,^[a] Michel Huché,^[a] and Gérard Jaouen^{*[a]}

We recently reported that a ferrocenyl diphenol butene derivative showed a very strong cytotoxic effect on both hormone-dependent and -independent breast cancer cell lines. In order to obtain more information about the structure–activity relationship in the cytotoxicity of small ferrocene compounds, we have prepared a series of simple unconjugated ferrocenyl diphenol complexes (ortho,para; meta,para; para,para). These compounds retain a reasonable to good affinity for both estrogen receptor types, with higher values for the β form, and superior binding for the para,para diphenol complex (RBA = 28%). In vitro these complexes exhibit significant cytotoxic effects on hormone-independent pros-

tate (PC3) and breast cancer cell lines (MDA-MB231), with IC_{50} values between 2.5 and 4.1 μ M. This effect is more marked with PC3, the ortho,para diphenol complex proving the most effective. On the hormone-dependent MCF7 breast cancer cell line, the observed effect seems to be the result of two components, one cytotoxic (antiproliferative), the other estrogenic (proliferative). Electrochemical studies show that the cytotoxic effect of the complexes correlates with the ease of oxidation of the ferrocene group. All these complexes are much less cytotoxic than the ferrocenyl diphenol butene derivative.

Introduction

Inspired by the success of inorganic Pt complexes,^[1] the use of coordination and organometallic compounds in the treatment of cancer has been an active field of study for the last two decades.^[2] Recently, the ruthenium compound NAMI-A (imidazolium-*trans*-tetrachloro(dimethylsulfoxide) imidazolium-ruthenium(II)) has successfully completed phase I clinical trials as an anti-metastatic drug,^[3] while KP1019 (imidazolium *trans*-[tetrachlorobisindazole ruthenate(II)]) entered phase I clinical trials in 2003.^[4] Progress has also been made in the development of antitumor gallium compounds: tris(3-hydroxy-2-methyl-4H-pyran-4-onato)gallium(III) (gallium maltolate) and tris(8-quinolinolato)gallium(III) (KP46) also entered phase I trials in 2003.^[5]

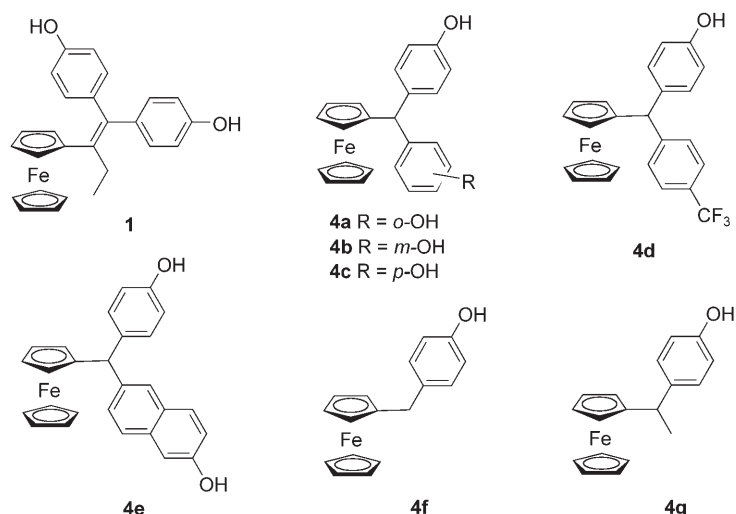
Cytotoxicity is also a property of some simple organometallic ferrocenium salts. The in vivo and in vitro antiproliferative activity of ferrocenium compounds against Ehrlich ascites tumor (EAT) cells was observed as early as 1985, although the insolubility in water of the corresponding neutral ferrocene compounds limited their efficacy.^[6] It has recently been demonstrated that ferrocenium salts are cytotoxic against MCF7 breast cancer cells, although the corresponding ferrocene compounds (derivatized with polar groups to increase water solubility) still exhibited no activity.^[7,8] The mechanism of cytotoxicity seems to occur, at least in part, by the Fenton reaction whereby ferrocenium cations promote DNA cleavage through the production of hydroxyl radicals.^[9] A recent study has shown an antiproliferative effect for iron(II) ferrocene compounds, in which the ferrocene itself yielded an antitumor effect in mice.^[10] Ferrocene–gold thiosemicarbazones have also shown modest antiproliferative activity against a human cervix

carcinoma cell line,^[11] although the mechanism of cytotoxicity for these rather complex molecules has not been explored.

We recently reported that the ferrocenyl diphenol butene derivative **1** (Scheme 1) showed a very strong cytotoxic effect against both hormone-dependent (MCF7) and -independent (MDA-MB231) breast cancer cell lines.^[12] This effect seems to arise from the combination of an easily oxidizable ferrocenyl group with a specific structural motif discussed below. In order to obtain information about the structure–activity relationship in the cytotoxicity of small ferrocene–phenol compounds, we tested the in vitro antiproliferative activity of a series of simple, unconjugated ferrocene–diphenol compounds, **4a–c**, on prostate and breast cancer cell lines. The synthesis, characterization, and determination of the relative binding affinities for the estrogen receptors are also reported, as well as electrochemical and molecular modeling studies for **4a–c** and for the analogues depicted in Scheme 1.

[a] Dr. E. Hillard, Dr. A. Vessières, Dr. F. Le Bideau, Dr. D. Plazuk, D. Spera, Dr. M. Huché, Prof. G. Jaouen
Laboratoire de Chimie et Biochimie des Complexes Moléculaires
UMR CNRS 7576
Ecole Nationale Supérieure de Chimie de Paris
11, rue Pierre et Marie Curie, 75231 Paris Cedex 05 (France)
Fax: (+33) 143-260-061
E-mail: gerard-jaouen@enscp.fr

[b] Dr. D. Plazuk
Present address:
Department of Organic Chemistry, University of Łódź
Narutowicza 68, 90-136 Łódź (Poland)



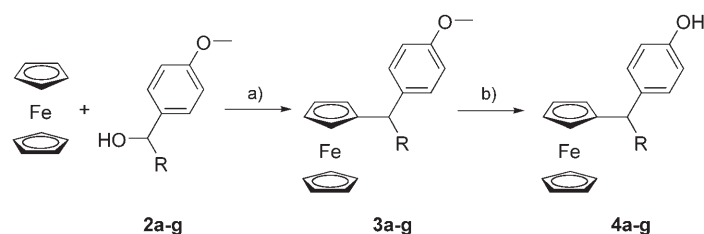
Scheme 1. Ferrocenyl phenol compounds studied in this report.

Results and Discussion

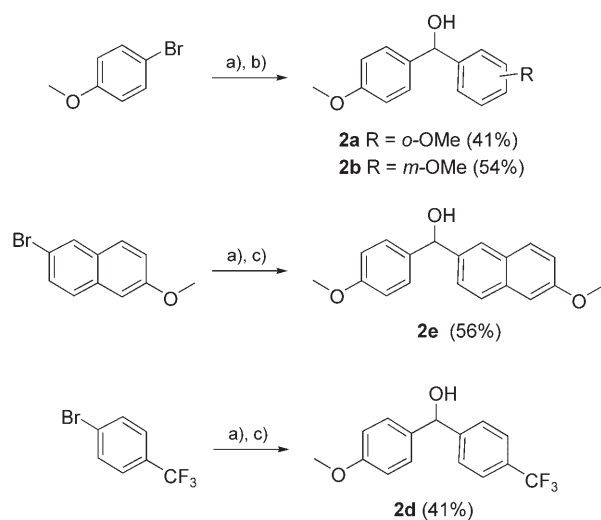
Synthesis

The synthesis of **4a–g** was outlined in a previous communication.^[13] Alcohols **2c, f, and g** are commercially available; **2a, b, d, and e** were obtained by the addition of organolithium reagents (prepared by halogen–metal exchange between the brominated derivatives and *n*-butyllithium) to the appropriate anisaldehydes (Scheme 2).

Compounds **3a–g** were synthesized by treatment of ferrocene with alcohols **2a–g** under very mild conditions (a solution of trifluoroacetic acid in dichloromethane at room temperature; Scheme 3). Under these conditions, di- or polysubstituted ferrocenes, previously obtained by using aluminum trichloride as a catalyst,^[14] were



Scheme 3. Reagents and conditions: a) (*p*-MeOC₆H₄)(R)CHOH, CF₃CO₂H, CH₂Cl₂, RT; b) BBr₃, CH₂Cl₂, RT; **3a**, (R = *o*-MeOC₆H₄); **4a**, (R = *o*-HOC₆H₄); **3b**, (R = *m*-MeOC₆H₄); **4b**, (R = *m*-HOC₆H₄); **3c**, (R = *p*-MeOC₆H₄); **4c**, (R = *p*-HOC₆H₄); **3d, 4d** (R = *p*-CF₃C₆H₄); **3e**, (R = 6-MeO-2-naphthyl); **4e**, (R = 6-OH-2-naphthyl); **3f, 4f** (R = H); **3g, 4g** (R = Me).



Scheme 2. a) *n*BuLi, −78 °C, THF, 1 h. b) *o*- or *m*-anisaldehyde, RT, 20 min. c) *p*-anisaldehyde, RT, 20 min.

only formed in low yields and were easily separated from the desired products, **3a–g**, by flash chromatography. The methoxy groups were then converted to the corresponding hydroxy groups by demethylation with boron tribromide to produce **4a–g** (yield: 36–63%).

Compound **1** was synthesized by a McMurry cross-coupling reaction between ferrocenyl ethyl ketone and the diphenol ketone, as previously described.^[15]

Biological studies

Measurement of the relative binding affinities (RBAs) of **4a–g** for the estrogen receptors, ER α and ER β . Biochemical studies were carried out on compounds **4a–g**, on a mixture of the two isomers where applicable, and compared to the reference complex **1** (Table 1). All the complexes were recognized by both

Table 1. Relative binding affinity values for 1 and 4a–g .			
	RBA for ER α ^[a]	RBA for ER β ^[a]	RBA(ER β)/RBA(ER α)
1	9.6 ± 0.9 ^[b]	16.3 ± 1.5 ^[b]	1.7
4a	2.1 ± 0.1	7.5 ± 0.5	3.6
4b	4.6 ± 0.1	15.5 ± 0.5	3.4
4c	18.2 ± 1.5	28 ± 2	1.5
4d	2.6 ± 0.1	7.8 ± 0.2	3.0
4e	3.8 ± 0.9	8.1 ± 0.4	2.1
4f	1.1 ± 0.1	3.5 ± 0.5	3.2
4g	5.2 ± 0.3	10.8 ± 0.8	2.1

[a] Mean of two experiments ± range. [b] Value from ref. [12]. Sheep uterine cytosol was used as a source of ER α and recombinant receptor for ER β .

estrogen receptor types. The RBA values obtained for ER β were significantly higher than those for ER α (ratio RBA(ER β)/RBA(ER α) between 1.5 and 3.6). The RBA values obtained for the mono- and diphenol complexes were similar, except for **4c** (18.2% for ER α and 28% for ER β), which were significantly higher than those for **1** (9.6 and 16.3%). RBA values are expressed relative to 17 β -estradiol (100%).

Table 2. Lipophilicity ($\log P_{o/w}$) and IC_{50} values for 4a–c PC3 and MDA-MB231 cells.			
	$\log P_{o/w}$	IC_{50} PC3 [μM] ^[a]	IC_{50} MDA-MB231 [μM] ^[a]
4a	4.9	2.5 ± 0.03	2.8 ± 0.1
4b	4.8	3.2 ± 0.3	4.1 ± 0.3
4c	4.7	3.1 ± 0.1	3.5 ± 0.02

[a] Mean of two experiments \pm range.

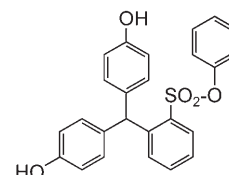
Determination of $\log P_{o/w}$ values. The lipophilicity of the complexes **4a–c** was determined by reversed-phase HPLC (Table 2). These values were similar to that found for **1** (5.0), and are significantly higher than the $\log P_{o/w}$ value of 17β -estradiol (3.5).^[15b]

In vitro study of diphenols **4a–c with prostate and breast cancer cell lines.** The effect of the compounds **4a–c** on cell proliferation was studied with three cancer cell lines—a hormone-independent prostate cancer cell line (PC3), and hormone-independent (MDA-MB231) and hormone-dependent (MCF7) breast cancer cell lines—and compared with the results obtained with $1 \mu\text{M}$ of **1**. The reference hormones were dihydrotestosterone (DHT) for prostate cancer cells and estradiol (E2) for breast cancer cells (Figure 1).

For the hormone-independent cell lines, PC3 and MDA-MB231, proliferation was tested at three concentrations of **4a–c**, and their IC_{50} values were calculated (Table 2). All of the ferrocenyl compounds exhibited significant antiproliferative effects, with complex **4a** proving the most effective. The compounds were slightly more effective on the prostate cancer cells than on the hormone-independent breast cancer cells. As expected, DHT and E2 had no effect on the hormone-independent cells, and the observed antiproliferative effect can be attributed to just the cytotoxic effect of the complexes.

For the hormone-dependent breast cancer cell line, MCF7, the effect of $1 \mu\text{M}$ of the compounds on cell growth was studied in the presence and absence of phenol red, a weak estrogen

classically used to monitor pH change in culture media (Figure 2). The estrogenic activity of phenol red is due to the presence of a minor (0.002%) impurity, bis(4-hydroxyphenyl)[2-(phenoxy-sulfonyl)-phenyl]methane, which has a high RBA value (50%) for the estrogen



receptor^[16] and a similar structural motif to those of **4a–c**. On MCF7 cells without phenol red, complexes **4b** and **4c** exhibited a significant proliferative effect (around 150%, E2 was 219%) while **4a** had practically no effect. Indeed, it was expected that these diphenol molecules with reasonable affinity for ER α would be estrogenic, as are their organic analogues.^[17] Therefore, the effect observed on the proliferation of hormone-dependent breast cancer cells must be considered to be the result of a combination of estrogenic (proliferative) and cytotoxic (antiproliferative) effects. In the presence of phenol red, there is a competition for binding to the estrogen receptor between these two estrogenic molecules. However, because the concentration of phenol red was much higher than that of the complexes, one would predict that the cytotoxic effect of the complexes would predominate over any estrogenic effect. This is exactly what is observed here: the antiproliferative effects of the complexes in the presence of phenol red were quite close to those observed on the MDA-MB231 cells.

The antiproliferative effects of the unconjugated complexes were significantly inferior to those observed for **1** on all cell lines. As previously reported, the IC_{50} value for **1** was found to be $0.6 \mu\text{M}$ ^[12] for the MDA-MB231 cell line, making **1** about 5–7 times more cytotoxic than **4a–c**.

Molecular modeling

Molecular mechanics studies were performed on compounds **1** and **4a–g**, to determine the stability of the optimum orientation in the ligand binding domain of the estrogen receptor.

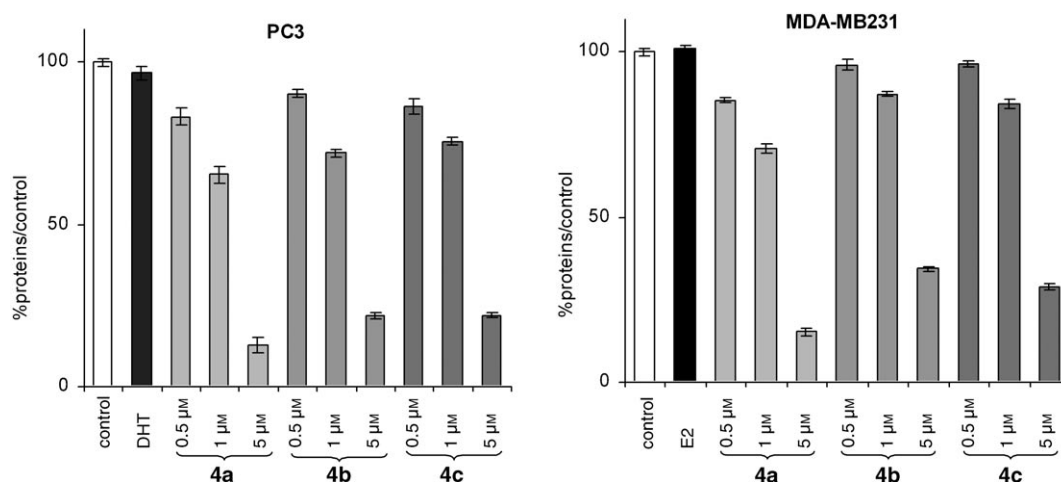


Figure 1. Study of the proliferative/antiproliferative effect of **4a–c** at different concentrations on PC3 (hormone-independent prostate cancer cells) and MDA-MB231 (hormone-independent breast cancer cells) after 5 days of culture. Comparison with the effect of 10 nM DHT (for PC3) and 10 nM E2 (for MDA-MB231). Representative data of one experiment performed twice with similar results (eight measurements \pm limits of confidence; $P = 0.1$, $t = 1.895$).

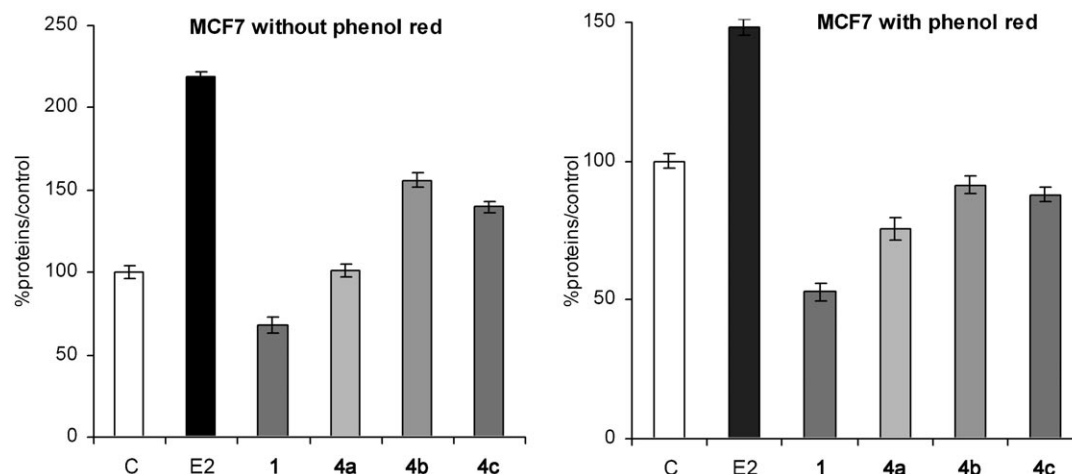


Figure 2. Study of the proliferative/antiproliferative effect of $1 \mu\text{M}$ of **1** and **4a–c** (C = control) on MCF7 (hormone-dependent breast cancer cells) after 5 days of culture. Comparison with the effect of 10 nM E2. Representative data of one experiment performed twice with similar results (eight measurements \pm limits of confidence; $P=0.1$, $t=1.895$).

We utilized the crystal structure of the ligand binding domain of human ER α bound to estradiol^[18] (for **1**) or diethylstilbestrol (DES; for **4a–g**).^[19] Only the amino acids forming the wall of the cavity were conserved, and the E2 or DES molecule was digitally replaced with the bioligand to be studied. All the heavy atoms of the cavity were immobilized, although the lateral chain of His524 was liberated for compound **1** due to the relatively large size of this molecule. This was justified by the fact that this part of the cavity has been shown to be flexible.^[20] An energy-minimization routine was then carried out with all of the heavy atoms immobilized except those of the bioligand, and possibly the His524 side chain, by using the Merck Molecular Force Field (MMFF) to determine the best position for the bioligand. Next, the affinity of the bioligand for the cavity was determined by using PM3 semiempirical methods. Calculations were performed for the bioligand–cavity combination, and for the cavity and the bioligand separately, with the latter two retaining the conformations they had in the molecular complex. This gave the ΔrH° energy for the reaction: bioligand + cavity \rightarrow molecular complex (Table 3).

For compound **1**, the modeling was initially carried out with the crystal structure containing E2 in the cavity. The cavity of the structure containing E2 is very similar to that containing DES, both in terms of volume and shape. The orientation of

compound **1** in the cavity is shown in Figure 3a. One of the hydroxyl groups forms hydrogen bonds with amino acids Arg394 and Glu353, while the ferrocene seems to have only a slight affinity (if any) for the imidazole of His524. The second phenol is oriented vertically in the slit of the cavity pointing toward Asp351 (not shown in the figure), without actually reaching it.

For compounds **4a–g**, the orientation is similar to that of compound **1**, with one phenol group engaging in hydrogen bonding interactions with Arg394 and Glu353, and the other phenol, CF₃, naphthol, or methyl group oriented toward Asp351. However, in **4a** and **b**, the hydroxyl group does not point directly up into space, but is oriented toward hydrophobic residues; this causes a slight destabilization relative to **4c** (Figure 3b). For compounds **4a–g**, the isomer that has the best ΔrH° value is the one in which the hydrogen atom is at the back of the molecule.

For additional precision, geometric optimizations for the *S* isomers of **4a–c** were performed by semiempirical (PM3) methods. For compound **4a**, the hydroxyl proton of the *ortho*-substituted phenol displays an association with the iron atom, with an Fe–H bond length of 2.6 \AA and a O–H–Fe angle of 168° , signifying a hydrogen bond. A DFT calculation on the isolated molecule yielded an Fe–H bond length of 2.0 \AA .

	Volume [\AA^3]	ΔrH° <i>R</i> isomer [kcal mol ⁻¹]	ΔrH° <i>S</i> isomer [kcal mol ⁻¹]	ΔrH° mean [kcal mol ⁻¹]
1	446	n/a	n/a	-18.6
4a	391	-14.9	-23.0	-19.0
4b	391	-15.2	-25.6	-20.4
4c	391	n/a	n/a	-27.7
4d	420	-27.1	-14.2	-20.7
4e	444	-23.8	-14.2	-19.0
4f	294	n/a	n/a	-19.0
4g	322	-19.0	-30.0	-24.5

Electrochemical studies

Because previous studies have linked cytotoxicity with the ferrocenium cation, electrochemical experiments were undertaken to determine if the oxidative chemistry differed between the strongly cytotoxic **1**, and the moderately cytotoxic **4a–c**. Cyclic voltamograms for compounds **1**, **4a–c**, and **4e–g** were obtained in both methanol and methanol/pyridine (6:1 v/v). Methanol was chosen to simulate an aqueous environment for these hydrophobic compounds, and the addition of pyridine allowed us to try to predict reactivity toward nucleophiles/bases of the electrochemically generated radical cations. In

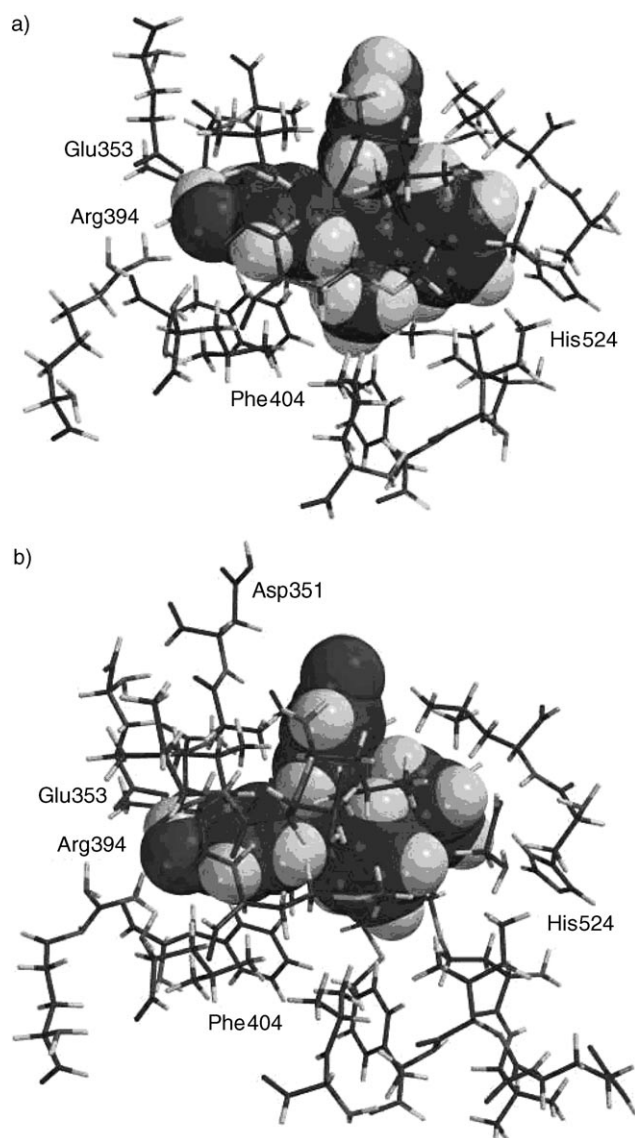


Figure 3. Molecular models for a) **1**, and b) **4c**. The bioligands are depicted as compact models of van der Waals sphere radii, and the amino acids that constitute the wall of the cavity are shown as stick drawings. The amino acids that interact with the bioligand are labeled.

methanol, all of the cyclic voltammograms showed a conventional and reversible ferrocene/ferrocenium couple, with additional higher-potential irreversible phenol oxidation waves for compounds **1**, **4b–c**, and **4e–f**. Phenol oxidation waves were not detected for compounds **4a** and **g**. With the addition of pyridine, the ferrocene/ferrocenium couples for compounds **4a–c** and **4e–g** shifted to slightly higher potentials, but were not qualitatively changed. For compound **1**, however, the ferrocene oxidation wave was intensified, the ferrocenium reduction wave disappeared, and the phenol oxidation wave exhibited a dramatic cathodic shift (Figure 4). While all the observed phenol oxidation waves shifted to lower potentials in the presence of pyridine, none of the displacements was as dramatic as that for compound **1** ($\Delta E=0.4$ V). The smaller observed shifts for compounds **4b**, **c**, **e**, and **f** ($\Delta E=0.1$ – 0.2 V) might

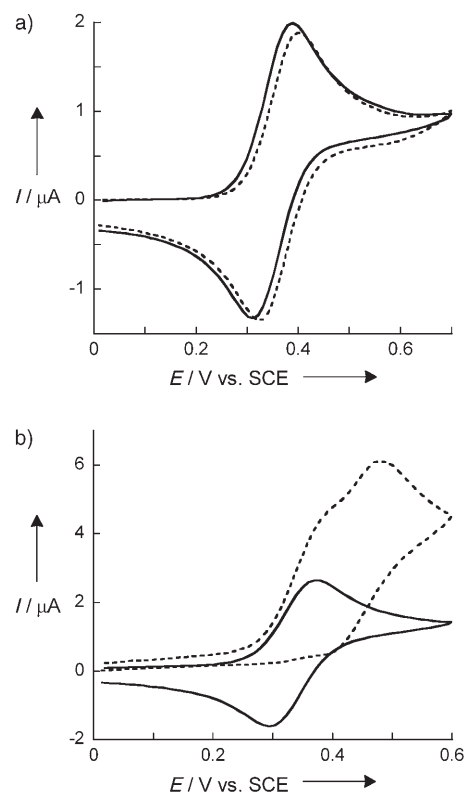


Figure 4. Cyclic voltammograms of a) **4c** and b) **1**. 2 mM in 0.1 M $\text{Bu}_4\text{NBF}_4/\text{MeOH}$ in the absence (—) and presence (---) of pyridine (1:6, v/v). Scan rate 0.5 V s^{-1} with a 0.5 mm diameter Pt electrode.

arise from the formation of hydrogen bonds with the added pyridine (Table 4).^[21]

Table 4. Standard oxidation potentials for **1**, **4a–c**, and **4e–g** vs. SCE.

	MeOH		MeOH/py	
	E_C°	$E_{2\text{nd wave}}^\circ$	E_{Fc}°	$E_{2\text{nd wave}}^\circ$
1	0.373(3)	0.88(3)	0.387(3)	0.480(3)
4a	0.379(3) ^[a]	n.o. ^[b]	0.399(3) ^[a]	0.98(2)
4b	0.400(3) ^[a]	1.17(2)	0.423(3) ^[a]	0.93(2)
4c	0.389(3) ^[a]	1.14(2)	0.406(3) ^[a]	0.85(1)
4e	0.406(4)	1.05(2)	0.424(4)	0.78(1)
4f	0.375(2)	v.b. ^[c]	0.385(2)	1.1(2) ^[c]
4g	0.377(3)	n.o. ^[b]	0.391(3)	1.0(1) ^[c]

[a] Mean of two experiments. Number in parentheses reflects the uncertainty in the last digit. [b] Not observed. [c] Very broad.

The results for **1** suggest an intramolecular electron transfer to the ferrocene moiety after the first electrochemical oxidation, causing regeneration of the Fe^{II} species. It is likely that the π system in **1** provides a conduit for electron transfer, and that the ferrocenium acts as an intramolecular oxidant of the phenol to yield possibly a reactive electrophilic quinoid. This might be the active species accounting for the cytotoxicity of this compound.^[22] Lacking a π system, the other compounds cannot mediate this electron transfer, and indeed no chemical

reduction of the electrochemically generated ferrocenium moiety was observed. Nonetheless, compounds **4a–c** showed significant cytotoxicity. That their antiproliferative effects correlate with the ease of oxidation of the ferrocene group suggests that this milder cytotoxicity might arise from Fenton chemistry, rather than the production of quinoid species. It has previously been observed that *o*-MeO-substituted benzylferrocenes are more easily oxidized than those with *p*-substitution.^[23]

Experimental Section

General comments: Starting materials were synthesized by using standard Schlenk techniques under argon. THF was dried and distilled over sodium benzophenone prior to use. Thin-layer chromatography was performed on silica gel 60 GF254. FTIR spectra were recorded on a BOMEM Michelson-100 spectrometer in a KBr plate. ¹H and ¹³C NMR spectra were acquired on Bruker 300 and 400 spectrometers with CDCl₃ as the solvent. Mass spectrometry was performed on a Nermag R 10-10C spectrometer. Melting points were measured by using a Kofler device. Elemental analyses were performed by the Regional Microanalysis Department of the Pierre and Marie Curie University. Molecular-modeling studies were carried out by utilizing Mac Spartan Pro, PC Spartan Pro, and Titan.^[25] Compounds **2c**, **f** and **g** were purchased from Aldrich.

Synthesis

General procedure for the preparation of benzyl alcohols: *n*BuLi (12.5 mL, *c* = 1.6; 20.0 mmol) was added to a solution of arylbromide (20 mmol) in THF (20 mL) at –78 °C. After 1 h, a solution of aryl aldehyde (20 mmol) in THF (5 mL) was added, the cold bath removed, and the reaction mixture was stirred for 20 min at room temperature. This was poured into water (20 mL), extracted with CH₂Cl₂ (5 × 25 mL), dried over MgSO₄, and concentrated. The alcohols were purified by flash chromatography (CH₂Cl₂).

General procedure for the Friedel–Crafts reaction: CF₃COOH (0.3 mL) was added to a solution of ferrocene (2 mmol) and benzyl alcohol (1 mmol) in CH₂Cl₂ (5 mL). The resulting mixture was stirred at room temperature for 20 min and poured into saturated NaHCO₃ (20 mL). The aqueous phase was extracted with CH₂Cl₂ (5 × 20 mL). The compounds were purified by flash chromatography (pentane/CH₂Cl₂ 1:1) and crystallized from petroleum ether.

General procedure for the demethylation: A solution of **3a–g** (1 mmol) in CH₂Cl₂ (5 mL) was treated at room temperature with a solution of BBr₃ (1 M) in CH₂Cl₂ (5 mL) for each methoxy group. The resulting mixture was stirred at room temperature until disappearance of the ferrocene (TLC control, 10–20 min), then poured into saturated NaHCO₃ (20 mL). After extraction with CH₂Cl₂, the products, **3a–g**, were isolated by flash chromatography (SiO₂, CH₂Cl₂/ethyl acetate 97:13). Solid products were dissolved in CH₂Cl₂ and recrystallized by the slow addition of pentane until precipitation occurred.

Characterization

(2,4'-Dimethoxybenzhydryl)alcohol (2a): Previously described, see ref. [26]. Yield: 41%.

(2,4'-Dimethoxybenzhydryl)ferrocene (3a): Yield: 47%; m.p.: 106 °C; ¹H NMR (300 MHz, CDCl₃): δ = 3.80 (s, 3H; OMe), 3.82 (s, 3H; OMe), 3.98 (s, 1H; C₅H₄), 7.07 (s, 6H; C₅H₄, Cp), 4.16 (s, 2H; C₅H₄), 5.59 (s, 1H; CH), 6.8–6.9 (m, 4H; Ph), 7.02 (d, *J* = 6.0 Hz, 1H; Ph), 7.0–7.3 ppm (m, 3H; Ph); ¹³C NMR (75 MHz, CDCl₃): δ = 43.0, 55.2, 55.4, 67.2, 67.7, 68.5, 68.7, 69.7, 92.2, 110.4, 113.1, 120.2, 127.1, 129.4, 129.8, 134.4, 136.9, 156.2, 157.6 ppm; IR (KBr): $\tilde{\nu}$ = 3100–2820, 2362,

1240 cm⁻¹; MS: 412 [M]⁺; elemental analysis calcd (%) for C₂₅H₂₄FeO₂: C 72.83, H 5.87; found: C 72.53, H 6.01.

(2,4'-Dihydroxybenzhydryl)ferrocene (4a): Yield: 46%; m.p.: 164 °C; ¹H NMR (300 MHz, CDCl₃): δ = 3.90 (s, 1H; C₅H₄), 4.05 (s, 5H; Cp), 4.10 (s, 1H; C₅H₄), 4.17 (s, 1H; C₅H₄), 4.18 (s, 1H; C₅H₄), 4.74 (s, OH), 4.81 (s, OH), 5.30 (s, CH), 6.6–6.8 (m, 4H; Ph), 6.6–6.9 (m, 1H; Ph), 6.96 (m, 1H; Oh), 7.0–7.2 ppm (m, 2H; Ph); ¹³C NMR (75 MHz, CDCl₃): δ = 45.4, 67.5, 68.1, 68.5, 68.8, 69.0, 91.1, 115.2, 116.2, 120.6, 127.7, 129.9, 131.7, 135.4, 153.0, 154.2 ppm; IR (KBr): $\tilde{\nu}$ = 3400, 1510, 1451, 1219 cm⁻¹; MS: 384 [M]⁺; elemental analysis calcd (%) for C₂₄H₂₀FeO₂: C 71.89, H 5.25; found: C 71.52, H 5.29.

(3,4'-Dimethoxybenzhydryl)alcohol (2b): Yield: 54%. Was identified by comparison with the published data.^[27]

(3,4'-Dimethoxybenzhydryl)ferrocene (3b): Yield: 55%, as an oil; ¹H NMR (300 MHz, CDCl₃): δ = 3.76 (s, 3H; OMe), 3.79 (s, 3H; OMe), 3.98 (s, 1H; C₅H₄), 4.03 (s, 6H; C₅H₄, Cp), 4.15 (s, 2H; C₅H₄), 5.08 (s, 1H; CH), 6.7–6.9 (m, 6H; Ph), 7.11 (d, *J* = 8.0 Hz, 2H; Ph), 7.19 ppm (t, *J* = 7.9 Hz, 2H; Ph); ¹³C NMR (75 MHz, CDCl₃): δ = 51.0, 55.1, 55.2, 67.6, 68.7, 77.2, 91.9, 110.9, 113.4, 114.8, 121.2, 128.9, 129.6, 137.2, 147.0, 157.9, 159.3 ppm; IR (CDCl₃): $\tilde{\nu}$ = 3093, 2963, 2928, 2838, 1601 cm⁻¹; MS: 412 [M]⁺; elemental analysis calcd (%) for C₂₅H₂₄FeO₂: C 72.83, H 5.87; found: C 72.55, H 5.80.

(3,4'-Dihydroxybenzhydryl)ferrocene (4b): Yield: 51%; m.p.: 80 °C; ¹H NMR (300 MHz, CDCl₃): δ = 3.98 (s, 1H; C₅H₄), 4.04 (s, 6H; C₅H₄, Cp), 4.17 (s, 2H; C₅H₄), 4.86 (s, OH), 4.89 (s, OH), 5.05 (s, 1H; CH), 6.60 (t, 1H; *J* = 3.0 Hz, Ph), 6.66 (d, *J* = 9.0 Hz, 1H; Ph), 6.6–6.9 (m, 3H; Ph), 7.06 (d, *J* = 9.0 Hz, 2H; Ph), 7.14 ppm (t, *J* = 9.0 Hz, 1H; Ph); ¹³C NMR (75 MHz, CDCl₃): δ = 50.8, 67.6, 67.7, 68.7, 91.7, 113.0, 114.9, 115.6, 121.3, 129.2, 129.9, 137.2, 147.3, 153.8, 155.2 ppm; IR (KBr): $\tilde{\nu}$ = 3433 (OH), 1613, 1595, 1512, 1234 cm⁻¹; MS: 384 [M]⁺, 291 [M–HOC₆H₄]⁺; elemental analysis calcd (%) for C₂₃H₂₀FeO₂·H₂O: C 68.67, H 5.51; found: C 69.02, H 5.37.

(4,4'-Dimethoxybenzhydryl)ferrocene (3c): Yield: 55%; m.p.: 131 °C; ¹H NMR (300 MHz, CDCl₃): δ = 3.77 (s, 6H; OMe), 3.97 (brs, 2H; C₅H₄), 4.02 (brs, 5H; Cp), 4.14 (brs, 2H; C₅H₄), 5.06 (brs, 1H; CH), 6.80 (d, *J* = 8.2 Hz, 4H; Ph), 7.07 ppm (d, *J* = 8.2 Hz, 4H; Ph); ¹³C NMR (75 MHz, CDCl₃): δ = 50.1, 55.2, 67.6, 68.0, 68.7, 92.5, 113.4, 129.6, 137.7, 157.8 ppm; IR (CDCl₃): $\tilde{\nu}$ = 3094, 2966, 2831, 1606 cm⁻¹; elemental analysis calcd (%) for C₂₅H₂₄FeO₂: C 72.83, H 5.87; found: C 72.56, H 5.93.

(4,4'-Dihydroxybenzhydryl)ferrocene (4c): Yield: 36%; m.p.: 50 °C (decomp.); ¹H NMR (300 MHz, [D₆]acetone): δ = 3.95 (t, *J* = 3.0 Hz, 2H; C₅H₄), 4.01 (s, 5H; Cp), 4.14 (t, *J* = 3.0 Hz, 2H; C₅H₄), 4.97 (s, 1H; CH), 6.73 (d, *J* = 8.6 Hz, 4H; Ph), 7.00 ppm (d, *J* = 8.6 Hz, 4H; Ph); ¹³C NMR (75 MHz, [D₆]acetone): δ = 50.8, 68.0, 69.3, 93.9, 115.4, 130.3, 137.7, 156.3 ppm; IR (CDCl₃): $\tilde{\nu}$ = 3599, 3504, 3093, 2978, 2868, 1600 cm⁻¹; MS: 384 [M]⁺; elemental analysis calcd (%) for C₂₃H₂₀FeO₂·H₂O: C 70.25, H 5.38; found: C 70.24, H 5.23.

(4-Methoxy-4'-trifluoromethylbenzhydryl)alcohol (2d): Yield: 41%. Was identified by comparison with published data.^[28]

(4-Methoxy-4'-trifluoromethylbenzhydryl)ferrocene (3d): Yield: 56%; m.p.: 125 °C; ¹H NMR (300 MHz, CDCl₃): δ = 3.82 (s, 3H; OMe), 3.97 (s, 1H; C₅H₄), 4.02 (s, 1H; C₅H₄), 4.05 (s, 5H; Cp), 4.20 (s, 3H; C₅H₄), 5.20 (s, 1H; CH), 6.87 (d, *J* = 9.0 Hz, 2H; Ph), 7.01 (d, *J* = 9.0 Hz, 2H; Ph), 7.30 (d, *J* = 9.0 Hz, 2H; Ph), 7.55 ppm (d, *J* = 9.0 Hz, 2H; Ar); ¹³C NMR (75 MHz, CDCl₃): δ = 51.0, 55.4, 67.9, 68.0, 68.7, 68.9, 77.3, 91.2, 113.7 ppm; IR (KBr): $\tilde{\nu}$ = 3100–2680, 1615, 1510, 1325 cm⁻¹; MS: 450 [M]⁺; 431 [M–F]⁺; elemental analysis calcd (%) for C₂₅H₂₁F₃FeO: C 66.69, H 4.70, found: C 66.72, H 4.83.

(4-Hydroxy-4'-trifluoromethylbenzhydryl)ferrocene (**4d**): Yield: 46%; m.p. 164 °C; ¹H NMR (300 MHz, CDCl₃): δ = 3.99–4.08 (m, 7H; C₅H₄, Cp), 4.23 (s, 2H; C₅H₄), 5.14 (s, 1H; CH), 6.77 (d, *J* = 9.0 Hz, 2H; Ph), 7.04 (d, *J* = 9.0 Hz, 2H; Ph), 7.29 (d, *J* = 9.0 Hz, 2H; Ph), 7.54 ppm (d, *J* = 9.0 Hz, 2H; Ph); ¹³C NMR (75 MHz, CDCl₃): δ = 50.8, 68.2, 68.9, 69.0, 69.2, 91.6, 126.0, 128.3 (q, *J* = 19 Hz), 128.7, 128.9, 129.8, 136.4, 149.2, 154.0 ppm; IR (KBr): $\tilde{\nu}$ = 3433 (OH), 1510, 1325 cm⁻¹.

4-Methoxy- α -(6-methoxy-2-naphthyl)benzyl alcohol (**2e**): Yield: 56%; m.p.: 78 °C; ¹H NMR (300 MHz, CDCl₃): δ = 3.96 (s, 3H; OMe), 4.08 (s, 3H; OMe), 6.09 (s, 1H; CH), 7.04 (d, *J* = 9.0 Hz, 2H; Ph), 7.2–8.0 ppm (m, 8H; Ph); ¹³C NMR (75 MHz, CDCl₃): δ = 55.2, 55.3, 75.8, 105.8, 113.9, 118.9, 124.8, 125.4, 127.1, 128.0, 128.7, 129.5, 134.0, 136.2, 139.2, 157.7, 159.0 ppm; IR (KBr): $\tilde{\nu}$ = 3328 (OH), 1606, 1508, 1249, 1169, 1031 cm⁻¹; MS: 294 [M]⁺, 277 [M–OH]⁺; elemental analysis calcd (%) for C₁₉H₁₈O₃: C 77.53, H 6.16; found: C 77.65, H 6.19.

(4-Methoxy- α -(6-methoxy-2-naphthyl)benzyl)ferrocene (**3e**): Yield: 47%; m.p.: 60 °C; ¹H NMR (300 MHz, CDCl₃): δ = 3.80 (s, 3H; OMe), 3.92 (s, 3H; OMe), 4.05 (s, 7H; C₅H₄, Cp), 4.19 (s, 2H; C₅H₄), 5.27 (s, 1H; CH), 6.83 (d, *J* = 9.0 Hz, 2H; Ph), 7.0–7.3 (m, 4H; Ph), 7.28 (dd, *J* = 9.0, 3.0 Hz, 1H; Ph), 7.53 (s, 1H; Ph), 7.66 ppm (t, *J* = 9.0 Hz, 2H; Ph); ¹³C NMR (75 MHz, CDCl₃): δ = 50.9, 55.2, 55.3, 67.5, 67.6, 68.7, 68.8, 92.2, 105.6, 113.4, 118.6, 126.4, 126.6, 128.0, 128.8, 129.3, 129.8, 133.1, 137.3, 140.7, 157.4, 157.9 ppm; IR (KBr): $\tilde{\nu}$ = 3100–2820, 1606, 1509 cm⁻¹; MS: 462 [M]⁺; elemental analysis calcd (%) for C₂₉H₂₆FeO₂: C 75.33, H 5.67; found: C 75.53, H 5.75.

(4-Hydroxy- α -(6-hydroxy-2-naphthyl)-benzyl)ferrocene (**4e**): Yield: 37%; m.p.: 220 °C (decomp.); ¹H NMR (300 MHz, [D₆]acetone): δ = 3.8–3.9 (m, 7H; C₅H₄, Cp), 4.04 (s, 2H; C₅H₄), 5.12 (s, 1H; CH), 6.63 (d, *J* = 9.0 Hz, 2H; Ph), 6.9–7.1 (m, 4H; Ph), 7.13 (d, *J* = 9.0 Hz, 1H; Ph), 7.3–7.5 (m, 2H; Ph), 7.55 ppm (d, *J* = 9.0 Hz, 1H; Ph); ¹³C NMR (75 MHz, [D₆]acetone): δ = 51.6, 68.2, 69.5, 109.6, 115.6, 119.1, 126.6, 127.3, 128.8, 129.2, 130.1, 130.6, 134.5, 137.2, 141.4, 155.9, 156.5 ppm; IR (KBr): $\tilde{\nu}$ = 3448 (OH), 1603, 1510, 1210 cm⁻¹; MS: 434 [M]⁺; elemental analysis calcd (%) for C₂₇H₂₂FeO₂·H₂O: C 71.69, H 5.35; found: C 71.64, H 4.99.

(4-Methoxybenzyl)ferrocene (**3f**): Yield: 50%. Was identified by comparison with the published data.^[23]

(4-Hydroxybenzyl)ferrocene (**4f**): Yield: 63%. Was identified by comparison with the published data.^[28]

(4-Methoxyphenyl)ferrocenylmethane (**3g**): Yield: 55% as an oil; ¹H NMR (300 MHz, CDCl₃): δ = 1.66 (d, *J* = 7.2 Hz, 3H; CH₃), 3.83 (s, 3H; OMe), 3.89 (q, *J* = 7.2 Hz, 1H; CH), 4.06 (brs, 1H; C₅H₄), 4.15 (brs, 1H; C₅H₄), 4.20 (brs, 1H; C₅H₄), 4.21 (brs, 5H; Cp), 4.26 (brs, 1H; C₅H₄), 6.88 (d, *J* = 8.7 Hz, 2H; Ph), 7.17 ppm (d, *J* = 8.7 Hz, 2H; Ph); ¹³C NMR (75 MHz, CDCl₃): δ = 22.6, 38.7, 55.0, 66.2, 66.8, 67.4, 67.7, 68.4, 94.6, 113.4, 127.8, 139.6, 157.6 ppm; MS: 320 [M]⁺, 305 [M–CH₃]⁺; elemental analysis calcd (%) for C₂₉H₂₆FeO₂: C 71.27, H 6.30; found: C 71.27, H 6.88.

(4-Hydroxyphenyl)ferrocenylmethane (**4g**): Yield: 56%; m.p.: 88 °C; ¹H NMR (300 MHz, CDCl₃): δ = 1.58 (d, *J* = 6.0 Hz, 3H; CH₃), 3.82 (q, *J* = 6.0 Hz, 1H; CH), 4.00 (s, 1H; C₅H₄), 4.10 (s, 1H; C₅H₄), 4.1–4.2 (m, 6H; C₅H₄, Cp), 4.20 (s, 1H; C₅H₄), 6.75 (d, *J* = 9.0 Hz, 2H; Ph), 7.05 ppm (d, *J* = 9.0 Hz, 2H; Ph); ¹³C NMR (75 MHz, CDCl₃): δ = 22.7, 38.9, 66.3, 66.9, 67.5, 67.8, 68.6, 94.7, 115.0, 128.2, 140.0, 153.6 ppm; IR (KBr): $\tilde{\nu}$ = 3526–3123 (m), 2968, 2878, 1611, 1510 cm⁻¹; MS: 307 [M+H]⁺.

Biochemical experiments

Materials: Stock solutions (1 × 10⁻³ M) of the compounds to be tested were prepared in DMSO and stored at 4 °C in the dark; under these conditions they are stable for at least two months. Serial dilutions in ethanol were prepared immediately prior to use. Dulbecco's modified eagle medium (DMEM, Gibco BRL), fetal calf serum (Dutscher, Brumath, France), glutamine, estradiol, and protamine sulfate (Sigma) were purchased. PC3, DU145, MCF7, and MDA-MB231 cells were obtained from the Human Tumor Cell Bank. Sheep uteri weighing approximately 7 g were obtained from a slaughterhouse (Mantes-la-Jolie, France), immediately frozen and stored in liquid nitrogen.

Determination of the relative binding affinity (RBA) of the compounds for ER α and ER β . RBA values for ER α were measured by using sheep uterine cytosol prepared in buffer A (0.05 M Tris-HCl, 0.25 M sucrose, 0.1% β -mercaptoethanol, pH 7.4 at 25 °C) as described previously.^[29] Er β (10 μ L, 3500 pmol mL⁻¹; Pan Vera, Madison, WI) was added to buffer B (16 mL; 10% glycerol, 50 mM Bis-Tris-propane pH 9, 400 mM KCl, 2 mM dithiothreitol, 1 mM EDTA, 0.1% bovine serum albumin) in a silanized flask. Aliquots (200 μ L) of ER α in glass tubes or ER β in polypropylene tubes were incubated for 3 h at 0 °C with [6,7-³H]-estradiol (2 × 10⁻⁹ M, specific activity 1.62 TBq mmol⁻¹, NEN Life Science, Boston, MA) in the presence of nine concentrations of the compounds to be tested. At the end of the incubation period, the free and bound fractions of the tracer were separated by protamine sulfate precipitation. The percentage reduction in binding of [³H]estradiol (Y) was calculated by using the logit transformation of Y (logit Y: ln[Y/(1–Y)]) versus the log of the mass of the competing steroid. The concentration of unlabeled steroid required to displace 50% of the bound [³H]estradiol was calculated for each steroid tested, and the results were expressed as RBA. (The RBA of estradiol is 100% by definition).

Measurement of octanol/water partition coefficient (log P_{o/w}) of the compounds. The log P_{o/w} values of the compounds were determined by reversed-phase HPLC on a C-8 column (nucleosil 5.C8, Macherey–Nagel, France) according to the method previously described by Minick^[30] and Pomper.^[31] Chromatographic capacity factors (*k'*) for each compound were measured at various concentrations in the range 85–60% methanol (containing 0.25% octanol) and an aqueous phase consisting of 0.15% *n*-decylamine in MOPS buffer (0.02 M; pH 7.4, prepared in octan-1-ol-saturated water). These capacity factors (*k'*) were extrapolated to 100% of the aqueous component to give the values of *k'*_w. log P_{o/w} (y) values were obtained from the formula log P_{o/w} = 0.13418 + 0.98452 log *k'*_w.

Culture conditions: Cells were maintained in a monolayer in DMEM with phenol red (Gibco BRL) supplemented with fetal calf serum (8–9%, Gibco BRL) and glutamine (2 mM, Sigma) at 37 °C under a 5% CO₂ air humidified incubator. For proliferation assays, cells were plated and incubated in DMEM (1 mL) with or without phenol red, supplemented with decomplemented and hormone-depleted fetal calf serum (10%) and glutamine (2 mM). The following day (D0) the same medium containing the compounds to be tested (1 mL) was added to the plates (final volume of alcohol: 0.1% ; 4 wells for each condition, one plate per day). After 3 days (D3), the incubation medium was removed and fresh medium containing the compounds was added. After 6 days (D6), or 5 days (D5) for PC3, the total protein content of the plate was analyzed by methylene blue staining. Cell monolayers were fixed for 1 h in methanol, stained for 1 h with methylene blue (1 mg mL⁻¹ in PBS), then washed thoroughly with water. HCl (1 mL, 0.1 M) was added, and the absorbance of each well was measured at 620 nm on a

Biorad spectrophotometer. The results are expressed as the percentage of protein relative to the control.

Electrochemical experiments: Cyclic voltammograms were obtained by using an Autolab PGStat potentiostat driven by GPES software,^[24] a platinum wire counter electrode, a 500 μm platinum disc working electrode, and an aqueous standard calomel reference electrode. Analyte solutions were 1–2 mM in MeOH with Bu_4NBF_4 supporting electrolyte (0.1 M).

Conclusion

The results obtained here show that ferrocene linked to a nanovector designed to target preferentially the estrogen receptor yields cytotoxic effects in vitro, but that its interaction with the estrogen receptor remains agonistic. However, the strongly cytotoxic compound **1** contains a motif favorable for electron transfer between the phenol and the organometallic moiety. Oxidation of the ferrocene seems to promote electron transfer from the phenol moiety, possibly leading to a cytotoxic quinone methide entity. This electron flow between the ferrocenium and phenol group is largely attenuated in compounds **4a–c**, and the antiproliferative effect is weaker (IC_{50} values about five times higher than that of **1**); this is consistent with that exhibited by ferrocenium compounds, whose cytotoxicity has been shown to arise by the Fenton reaction.^[6b]

The approach presented here illustrates the contribution that the emerging field of bioorganometallic chemistry^[32] can bring to current oncology research. Certain tumors are characterized by intracellular accumulation of reactive oxygen species such as $\text{O}_2^{\cdot-}$, HO^\cdot , and H_2O_2 , a consequence of mitochondrial dysfunction.^[33] Moreover, the second estrogen receptor, $\text{ER}\beta$, which has been shown to be localized to the mitochondria,^[34] has been detected in the various cell lines studied here.^[15b,35]

The good recognition for $\text{ER}\beta$, coupled with a putative oxidative cytotoxic pathway, suggests that these compounds are potential drug candidates for hormone-independent cancers of the breast and prostate, although other biological targets cannot be excluded at this early stage. The approach of combining the idea of biological targeting with a chemical reaction specific to cancer cells offers new therapeutic strategies in cancer treatment, especially in light of the problem of drug resistance.

Acknowledgements

We thank A. Cordaville and M. A. Plamont for technical assistance. E.A.H. thanks the NSF (grant no. 0302042) for financial support, and Prof. Christian Amatore for use of his electrochemistry equipment and helpful discussions. D.S. and D.P.'s stay in Paris was supported through a European Community Marie Curie Fellowship (HMPT-CT-2000-00186).

Keywords: antitumor agents · bioorganometallic chemistry · iron · medicinal chemistry · phenols

- [1] a) B. Lippert, *Cisplatin: "Chemistry and Biochemistry of a Leading Anti-cancer Drug"*, Wiley, New York, **1999**; b) M. A. Jakupec, M. Galanski, B. K. Keppler, *Rev. Physiol. Biochem. Pharmacol.* **2003**, *146*, 1–54.
- [2] M. J. Clarke, F. Zhu, D. R. Frasca, *Chem. Rev.* **1999**, *99*, 2511–2533.
- [3] a) G. Sava, S. Zorzet, C. Turrin, F. Vita, M. Soranzo, G. Zabucchi, M. Cocchiello, A. Bergamo, S. DiGiovine, G. Pezzoni, L. Sartor, S. Garbisa, *Clin. Cancer Res.* **2003**, *9*, 1898–1905; b) J. M. Rademaker-Lakhai, D. van den Bongard, D. Pluim, J. H. Beijnen, J. H. Schellens, *Clin. Cancer Res.* **2004**, *10*, 3717–3727.
- [4] S. Kapitza, M. Pongratz, M. A. Jakupec, P. Heffeter, W. Berger, L. Lackinger, B. K. Keppler, B. Marian, *J. Cancer Res. Clin. Oncol.* **2005**, *131*, 101–110.
- [5] a) M. A. Jakupec, B. K. Keppler, *Curr. Top. Med. Chem.* **2004**, *4*, 1575–1583; b) M. A. Jakupec, B. K. Keppler, *Met. Ions Biol. Syst.* **2004**, *42*, 425–462.
- [6] a) P. Köpf-Maier, H. Köpf, E. W. Neuse, *J. Cancer Res. Clin. Oncol.* **1984**, *108*, 336–340; b) P. Köpf-Maier, *Z. Naturforsch.* **1985**, *40*, 843–846.
- [7] a) D. Osella, M. Ferrali, P. Zanella, F. Laschi, M. Fontani, C. Nervi, G. Cavigliolo, *Inorg. Chim. Acta* **2000**, *306*, 42–48; b) G. Tabbi, C. Cassino, G. Cavigliolo, D. Colangelo, A. Ghiglia, I. Viano, D. Osella, *J. Med. Chem.* **2002**, *45*, 5786–5796.
- [8] E. W. Neuse, F. Kanzawa, *Appl. Organomet. Chem.* **1990**, *4*, 19–26.
- [9] H. Tamura, M. Miwa, *Chem. Lett.* **1997**, *11*, 1177–1178.
- [10] R. Kovjazin, T. Eldar, M. Patya, A. Vanichkin, H. M. Lander, A. Novogrodsky, *FASEB J.* **2003**, *17*, 467–469.
- [11] J. S. Casas, M. V. Castaño, M. C. Cifuentes, J. C. García-Monteagudo, A. Sánchez, J. Sordo, U. Abram, *J. Inorg. Biochem.* **2004**, *98*, 1009–1016.
- [12] A. Vessières, S. Top, P. Pigeon, E. Hillard, L. Boubeker, D. Spera, G. Jaouen, *J. Med. Chem.* **2005**, *48*, 3937–3940.
- [13] D. Plazuk, A. Vessières, F. Le Bideau, G. Jaouen, J. Zakrzewski, *Tetrahedron Lett.* **2004**, *45*, 5425–5427.
- [14] E. W. Neuse, D. S. Trifan, *J. Am. Chem. Soc.* **1962**, *84*, 1850–1856.
- [15] a) G. Jaouen, S. Top, A. Vessières, G. Leclercq, J. Quivy, L. Jin, A. Croisy, C. R. Acad. Sci. Ser. Ilc **2000**, *3*, 89–93; b) S. Top, A. Vessières, G. Leclercq, J. Quivy, J. Tang, J. Vaissermann, M. Huché, G. Jaouen, *Chem. Eur. J.* **2003**, *9*, 5223–5236.
- [16] a) Y. Berthois, J. A. Katzenellenbogen, B. S. Katzenellenbogen, *Proc. Natl. Acad. Sci. USA* **1986**, *83*, 2496–2500; b) R. D. Bindal, J. A. Katzenellenbogen, *J. Med. Chem.* **1988**, *31*, 1978–1983.
- [17] A. Rivas, M. Lacroix, F. Olea-Serrano, I. Laios, G. Leclercq, N. Olea, *J. Steroid Biochem. Mol. Biol.* **2002**, *82*, 45–53.
- [18] a) A. M. Brzozowski, A. C. Pike, Z. Dauter, R. E. Hubbard, T. Bonn, O. Engström, L. Öhman, G. L. Greene, J. Å. Gustafsson, M. Carlquist, *Nature* **1997**, *389*, 753–758; b) A. C. Pike, A. M. Brzozowski, R. E. Hubbard, T. Bonn, A. G. Thorsell, O. Engström, J. Ljunggren, J. Å. Gustafsson, M. Carlquist, *EMBO J.* **1999**, *18*, 4608–4618.
- [19] A. K. Shiau, D. Barstad, P. M. Loria, L. Cheng, P. J. Kushner, D. A. Agard, G. L. Greene, *Cell* **1998**, *95*, 927–937.
- [20] R. N. Hanson, E. Napolitano, R. Fiaschi, *J. Med. Chem.* **1998**, *41*, 4686–4692.
- [21] Y. Fang, L. Liu, Y. Feng, X. S. Li, Q. X. Guo, *J. Phys. Chem. A* **2002**, *106*, 4669–4678.
- [22] The electrochemical results for compounds **1** and **4a–c** have been previously reported in E. A. Hillard, A. Vessières, L. Thouin, G. Jaouen, C. Amatore, *Angew. Chem.* **2006**, *118*, 291–296; *Angew. Chem. Int. Ed.* **2006**, *45*, 285–290. A second series of experiments was performed for this article; this accounts for the slight variation in reported oxidation potentials.
- [23] M. Asahara, S. Natsume, H. Kurihara, T. Yamaguchi, T. Erabi, M. Wada, *J. Organomet. Chem.* **2000**, *601*, 246–252.
- [24] General Purpose Electrochemical System, Version 4.8, EcoChemie B. V., Utrecht (The Netherlands).
- [25] Wavefunction Society, Irvine, CA (USA).
- [26] A. M. Choudhury, K. Schofield, R. S. Ward, *J. Chem. Soc. C* **1970**, 2543–2547.
- [27] G. E. Job, A. Shvets, W. H. Pirkle, S. Kuwahara, M. Kosaka, Y. Kasai, H. Tajiri, K. Fujita, M. Watanabe, N. Harada, *J. Chromatogr. A* **2004**, *1055*, 41–53.
- [28] T. V. Pham, R. A. McClelland, *Can. J. Chem.* **2001**, *79*, 1887–1897.
- [29] A. Vessières, S. Top, A. A. Ismail, I. S. Butler, M. Louër, G. Jaouen, *Biochemistry* **1988**, *27*, 6659–6666.

- [30] D. J. Minick, J. H. Frenz, M. A. Patrick, D. A. Brent, *J. Med. Chem.* **1988**, *31*, 1923–1933.
- [31] M. G. Pomper, H. VanBrocklin, A. M. Thieme, R. D. Thomas, D. O. Kiese-wetter, K. E. Carlson, C. J. Mathias, M. J. Welch, J. A. Katzenellenbogen, *J. Med. Chem.* **1990**, *33*, 3143–3155.
- [32] G. Jaouen, *Bioorganometallics*, Wiley-VCH, Weinheim, **2005**.
- [33] H. Pelicano, D. Carney, P. Huang, *Drug Resist. Updates* **2004**, *7*, 97–110.
- [34] a) S. H. Yang, R. Liu, E. J. Perez, Y. Wen, S. M. Stevens, T. Valencia, M. Brun-Zinkernagel, L. Prokai, Y. Will, J. Dykens, P. Koulen, J. W. Simpkins, *Proc. Natl. Acad. Sci. USA* **2004**, *101*, 4130–4135; b) J. Chen, M. Eshete, W. Alworth, J. Yager, *J. Cell. Biochem.* **2004**, *93*, 358–373.
- [35] G. Jaouen, S. Top, A. Vessières, G. Leclercq, M. J. McGlinchey, *Curr. Med. Chem.* **2004**, *11*, 2505–2517.

Received: September 1, 2005

Published online on April 11, 2006